

Article

Revealing the Impact of COVID-19 on Urban Residential Travel Structure Based on Floating Car Trajectory Data: A Case Study of Nantong, China

Fei Tao ^{1,2,†} , Junjie Wu ^{1,†}, Shuang Lin ^{1,†}, Yaqiao Lv ¹, Yu Wang ¹ and Tong Zhou ^{1,3,4,*} 

¹ School of Geographical Sciences, Nantong University, Nantong 226007, China

² Department of Land Surveying and Geo-Informatics, The Hong Kong Polytechnic University, Hong Kong, China

³ State Environmental Protection Scientific Observation and Research Station for Ecological Environment of Lake Hulun Wetland, Hulunbuir 021000, China

⁴ Jiangsu Yangtze River Economic Belt Research Institute, Nantong 226007, China

* Correspondence: zhoutong@ntu.edu.cn; Tel.: +86-135-8521-7135

† These authors equally contributed to the work.

Abstract: The volume of residential travel with different purposes follows relatively stable patterns in a specific period and state; therefore, it can reflect the operating status of urban traffic and even indicate urban vitality. Recent research has focused on changes in the spatiotemporal characteristics of urban mobility affected by the pandemic but has rarely examined the impact of COVID-19 on the travel conditions and psychological needs of residents. To quantitatively assess travel characteristics during COVID-19, this paper proposed a method by which to determine the purpose of residential travel by combining urban functional areas (UFAs) based on machine learning. Then, the residential travel structure, which includes origin–destination (OD) points, residential travel flow, and the proportion of flows for different purposes, was established. Based on taxi trajectory data obtained during the epidemic in Nantong, China, the case study explores changes in travel flow characteristics under the framework of the residential travel structure. Through comparison of the number and spatial distribution of OD points in the residential travel structure, it is found that residential travel hotspots decreased significantly. The ratios of commuting and medical travel increased from 43.8% to 45.7% and 7.1% to 8.1%, respectively. Conversely, the ratios of other travel types all decreased sharply. Moreover, under Maslow’s hierarchy of needs model, further insights into the impacts of COVID-19 on changes in residential psychological needs are discussed in this paper. This work can provide a reference for decision makers to cope with the change in urban traffic during a public health emergency, which is beneficial to the sustainable healthy development of cities.

Keywords: COVID-19; residential travel structure; machine learning; urban functional area; taxi trajectory; remote sensing



Citation: Tao, F.; Wu, J.; Lin, S.; Lv, Y.; Wang, Y.; Zhou, T. Revealing the Impact of COVID-19 on Urban Residential Travel Structure Based on Floating Car Trajectory Data: A Case Study of Nantong, China. *ISPRS Int. J. Geo-Inf.* **2023**, *12*, 55. <https://doi.org/10.3390/ijgi12020055>

Academic Editors: Hartwig Hochmair and Wolfgang Kainz

Received: 17 November 2022

Revised: 1 February 2023

Accepted: 5 February 2023

Published: 8 February 2023



Copyright: © 2023 by the authors. Licensee MDPI, Basel, Switzerland. This article is an open access article distributed under the terms and conditions of the Creative Commons Attribution (CC BY) license (<https://creativecommons.org/licenses/by/4.0/>).

1. Introduction

A local outbreak of pneumonia was detected in Wuhan, China, in December 2019 [1]. Later, it was found that the outbreak was due to a novel coronavirus, named severe acute respiratory syndrome coronavirus 2 (SARS-CoV-2) by the International Committee on Taxonomy of Viruses (ICTV) [2,3]. Since there was an absence of specific drugs and vaccines for this disease at the beginning of the pandemic, maintaining social distancing was the only way to reduce the spread of COVID-19 from person to person [4,5]. The governments of different countries adopted various policies to contain the pandemic; the most common was the lockdown policy [6,7]. The implementation of isolation policies dramatically limited residential travel for certain travel purposes [8,9], resulting in changes in the numbers and spatial distribution of origin–destination (OD) points and the proportions of different

directed residential travel flows with specific purposes in the residential travel structure. Studying these changes before and after the pandemic outbreak is of great significance for controlling the spread of disease transmission precisely [10] and promoting the sustainable healthy development of the region.

Social sensing data are a data resource with one important feature: the sensors of these data are individuals [11]. Nowadays, social sensing data from multiple sources (e.g., taxi data, mobile phone records, smart card data, social media check-in data, digital maps, etc.) contain rich information about spatial interactions and place semantics [11,12], and they are widely applied to understand urban environments from a human cognition perspective via various feature extraction methods during the pandemic. Many scholars have studied travel mode using social sensing data during COVID-19 [13–16], and studies are showing that the usage of public transportation has decreased significantly [17,18]. Hua found that bicycle sharing has been greatly impacted by COVID-19, with trips decreasing by 72–82% [19]. Since the trip distance on a shared bicycle is relatively limited and it is often used as a transfer transit tool during a long journey [20], a shared bicycle cannot accurately reflect the starting and ending points of travel. One study noted that the impact on the use of buses during the pandemic was larger than that on other kinds of traffic [21], so the bus data during COVID-19 cannot fully reflect the characteristics of residential flow. Taxi trajectory data can effectively reflect the origin and destination of travel [22], and they have the characteristic of continuous operation for 24 h [23]. Compared to other social sensing data, taxi trajectory data can reflect the mobility of residents from a small scale [24]; therefore, the origin–destination flows extracted from taxi trajectory data can reflect the similarities and differences in travel behavior before and after COVID-19.

It is essential to recognize the travel purpose to study the changes in residential travel characteristics during COVID-19. Points of interest (POI) data have been frequently utilized to determine the travel purpose in previous studies [25–27]. Furletti et al. used trajectory data and POI data to match drop-off points with visited POIs to determine travel purposes [28]. By matching POI data from the Google Places API with historical Twitter data, the popularity of each POI can be obtained to infer the travel purpose [29]. Luo et al. developed a hybrid data approach using taxi operational data and POI data to estimate travel purposes [30]. However, when there are multiple categories of POI around the drop-off points in the trajectory, it is difficult to determine the residential travel purpose [31,32]. Therefore, urban functional areas (UFAs) were used to determine the travel purpose in this paper by marking the trajectory data with different attributes of UFAs, which can improve the accuracy of determining the travel purpose.

Research on residential travel with different purposes has mainly focused on the analysis of a single travel purpose during the COVID-19 outbreak [33]. Several studies focusing on changes in commuting travel [34,35] or tourism travel [36,37] under the lockdown were carried out based on taxi data. However, there was no overall consideration of changes in residential travel with different purposes during COVID-19, such as commuting travel, medical travel, shopping travel, and other travel flows simultaneously. However, current research mostly focuses on changes in the psychological needs of a particular group under the background of the pandemic [38,39], such as the impact of the pandemic on the psychological needs of tourists [40]. However, the changes in multiple residential psychological needs during the pandemic that are hidden behind the residential mobility data are ignored. Therefore, in this study, tourism travel, shopping, commuting travel, business travel, and medical travel are incorporated into the residential travel structure, and changes in residential psychological needs based on Maslow's hierarchy of needs model are analyzed.

During the past decades, transport, Information and Communication Technologies (ICTs), and energy constitute the smart city pillars [41,42]. Research on residential travel is one of the emerging directions in the field of transportation [43]. The location and duration of the trip can be tracked more accurately through taxi trajectory data, thereby updating the traditional data obtaining method of questionnaires [44,45]. As more and

more urban cabs are equipped with navigation positioning and communication devices, research on residents' travel based on FCD data has gradually become a hot research issue in smart cities.

The main objectives of this work were as follows: (1) to determine residential travel purposes, the attributes of pick-up and drop-off points were identified according to six types of UFAs; (2) to reveal the spatiotemporal variation characteristics of residents' travel volume, the temporal variations in OD points and spatial variation in travel hotspots were analyzed; (3) to explain the impact of the pandemic, the proportion of directed travel and the fluctuations of the travel purpose were compared for the five periods of COVID-19; (4) to analyze the psychological statuses of the residents during the pandemic, the changes in the various travel needs were analyzed according to Maslow's hierarchy of needs model. Since the UFA data and taxi data can be continually updated, the travel behavior analysis based on the residential travel structure can help decision makers assess the health status of a city and adjust the control measures during major public health emergencies in the future.

2. Materials and Methods

2.1. Study Area

A city district was selected as the study area (Figure 1). Chongchuan District is located at $31^{\circ}58'48''$ N, $120^{\circ}53'42''$ E, in Nantong, Jiangsu Province, China, on the southeast coast of Jiangsu Province and the north bank of the Yangtze River estuary. Its total area is around 215 km². By 2020, the population was 7.318 million and the gross domestic product (GDP) was 1.00363 trillion Chinese Yuan. Since the subway is still under construction, taxis are one of the main choices for residential travel. Currently, Nantong city has a total of 1400 taxis in operation.

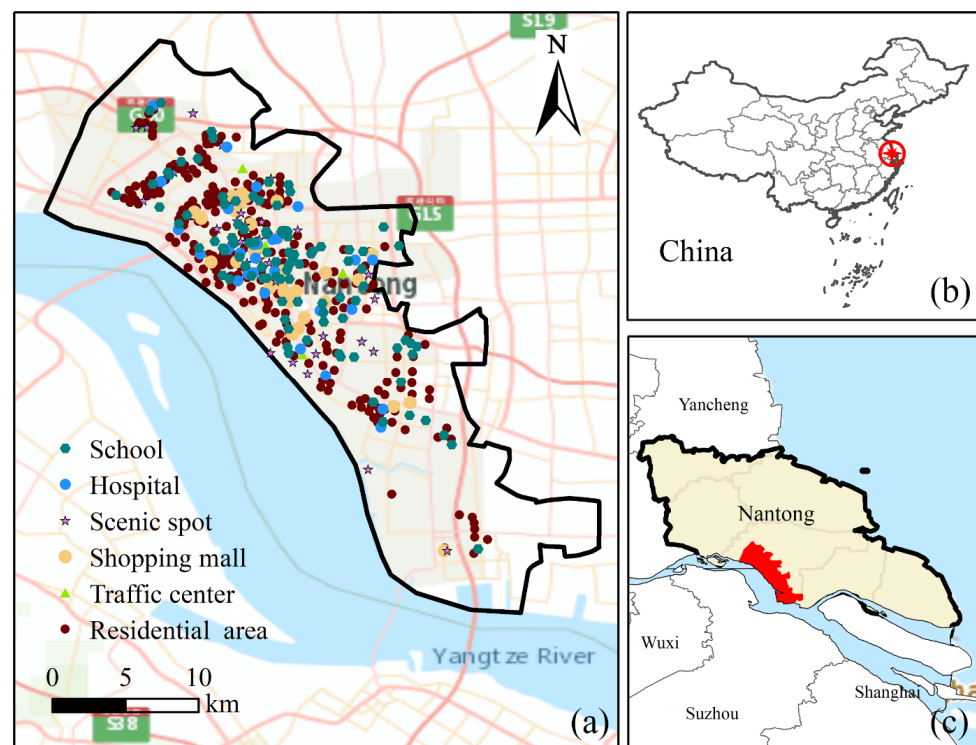


Figure 1. Study area. (a) Chongchuan District and marked points with attributes of UFAs, (b) map of China, (c) Nantong City.

2.2. Data Source and Description

2.2.1. Taxi Trajectory Data

As one of the most important big data sources in respect to social–spatial perception [46], taxi trajectory data were used to extract the OD matrix and to establish the residential travel structure. GPS trajectory data, whose positioning mode is single-point positioning (SSP), were provided by the Nantong Taxi Management System from December 2019 to March 2020. The original data contain license plate numbers, phone numbers, time, longitude and latitude, speed, direction, and passenger status.

The license plate number and phone number uniquely identify each taxicab. Time represents the moment when the tracking point in the trajectory is recorded. Longitude and latitude indicate the coordinates of the tracking point. Speed is a floating value that records the instantaneous velocity of the current taxi. Direction indicates the eight directions in which vehicles are driving. Passenger status denotes whether a taxi is occupied; this is a Boolean-type variable with a value of 0 when the car is empty.

2.2.2. Remote Sensing Data

To identify the attributes of UFAs, remote sensing images of Chongchuan District from Google Maps were used. Images were obtained from December 2019 to March 2020, including three RGB bands with a resolution of 0.5 m. To ensure the accuracy of the experiment, the images were preprocessed via radiometric calibration and fast line-of-sight atmospheric analysis of hypercubes (FLAASH) atmospheric correction [47] using the PIE-Basic platform.

2.3. Methodology

Due to the uncertainty in the study of residential travel, based on the statistical methods, the experiments in this paper were carried out based on the following theoretical hypotheses. First, the path of the cab from the pick-up point to the neighboring drop-off point was regarded as a complete travel path for the residents. Secondly, the social function attributes of the pick-up and drop-off points determined by UFA represent the travel purpose of residents. This research was divided into the following four parts, as shown in Figure 2. The first part involved the preprocessing of the taxi trajectory data and remote sensing images. The pick-up points and drop-off points were extracted, and attributes of UFAs were identified by machine learning. The second part involved determining the residential travel purposes and combining the OD points in the residential flow under the background of UFAs. The residential travel purposes were divided into tourism travel, shopping, commuting travel, business travel, medical travel, and random elastic travel. The third part involved analyzing the spatiotemporal characteristics of residential travel volume. Urban hotspots of travel were analyzed, and a coupling analysis between marked points with attributes of UFAs and the density of residential travel was conducted. The fourth part included the analysis of the directed travel and acquisition of proportions of different travel purposes in the residential travel structure. Finally, the changes in residential psychological needs before and after COVID-19 were analyzed under Maslow's hierarchy of needs model.

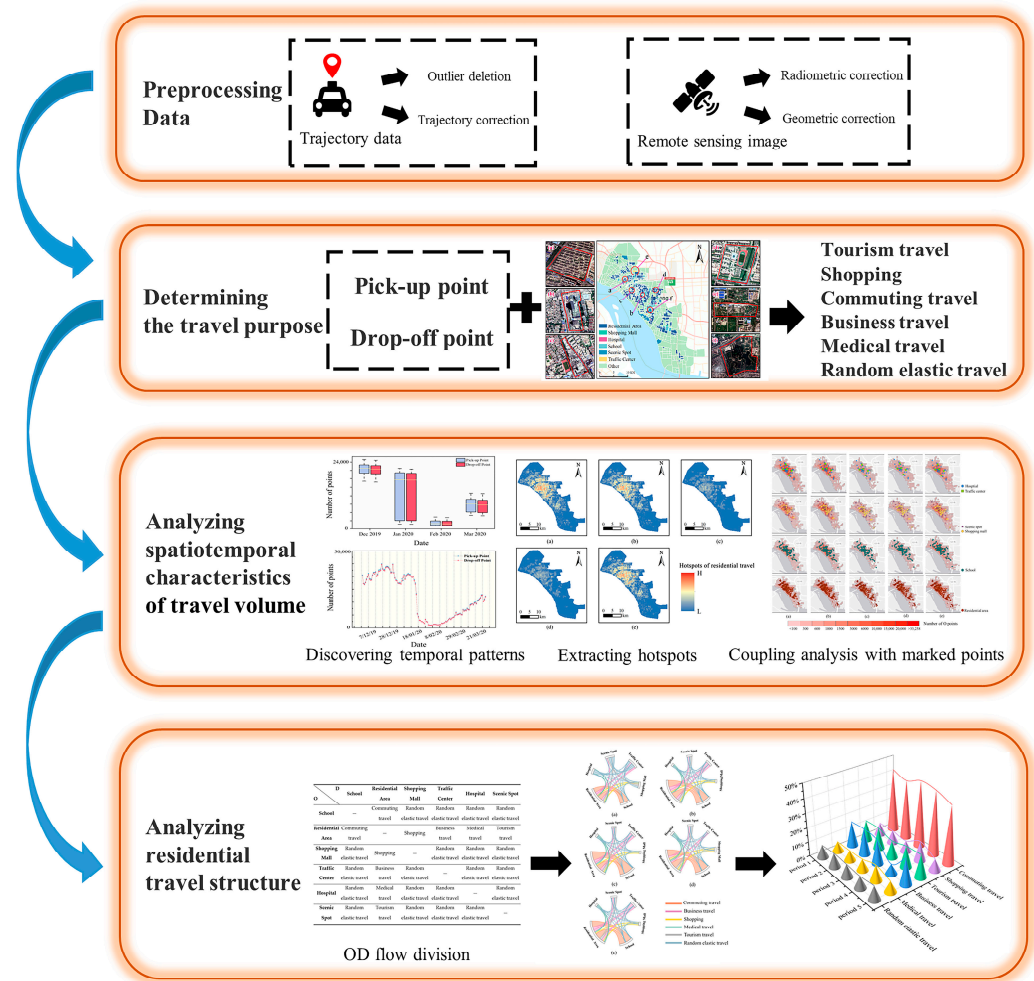


Figure 2. Framework of this paper. Marked points represent the points with urban functional area attributes; OD flow represents the origin–destination flow.

2.3.1. Calibration of Pick-Up and Drop-Off Points

The spatial accuracy of trajectory data obtained by the Beidou Navigation Satellite System (BDS) is about 5 to 10 m in the Asia–Pacific region. Theoretically, the signal point SP_i is obtained every 30 s during driving, and multiple consecutive signal points can reflect the taxi trajectory from SP_i to SP_n . According to the passenger status, the pick-up points and drop-off points were extracted. When the status changed from empty to occupied, the point was marked as the pick-up point, and vice versa for the drop-off point.

In the actual situation, the spatial error between the recorded pick-up point and the real one is relatively small and can be ignored, because the taxi driver will start the fee meter after the passenger gets in the taxi. However, some drivers are accustomed to stopping the fee meter in advance before reaching the destination, resulting in a large spatial error between the recorded drop-off point and the real one. Hence, when the status of recorded points changed from occupied to empty and the distance between the two points was less than 50 m, these kinds of recorded points were marked as drop-off points, and the distance formula is shown below.

$$dis = R \cdot \arccos[\cos \beta_1 \cos \beta_2 \cos(\alpha_1 - \alpha_2) + \sin \beta_1 \sin \beta_2] \tag{1}$$

where β_1 and β_2 represent the latitude angle of the pick-up and drop-off points, respectively; α_1 and α_2 represent the longitude angles of the pick-up and drop-off points, respectively; and R is the radius of the Earth.

2.3.2. Recognition of UFAs

UFAs were used to identify the trajectory OD points and determine the residential travel purpose. To recognize the attributes of UFAs, a trajectory sub-model $\Psi(T_i)$ and image sub-model $\Phi(I_i)$ were constructed, respectively, by coupling the taxi trajectory data and remote sensing images using machine learning and deep learning methods. Firstly, the trajectory sub-model was established by extracting the time-frequency series of the pick-up and drop-off points of each block, then the k-means++ and k-nearest-neighbor (kNN) algorithms were used to identify the attributes of the UFAs. When the trajectory data cannot provide effective decision-making due to the low amount of information, the sub-model of the image can be used to identify the attributes of UFAs, using a residual neural network (MLC-ResNets) and you only look once (YOLO) v3 to identify the attributes of the image.

The integration model $\Gamma(STET_i, T_i, I_i)$ was used to realize the identification of attributes of UFAs. If $STET$ was greater than or equal to the threshold ϵ , the trajectory sub-model $\Psi(T_i)$ was used; otherwise, the image sub-model $\Phi(I_i)$ was used. The formula is defined as follows [48].

$$\Gamma(STET_i, T_i, I_i) = \mathbb{I}_{(STET_i \geq \epsilon)} \Psi(T_i) + \mathbb{I}_{(STET_i < \epsilon)} \Phi(I_i) (i = 1, 2, \dots, n) \quad (2)$$

where n represents the number of blocks, T_i represents the trajectory data in block i , I_i represents the satellite image of block i , and $\mathbb{I}_{(condition)}$ refers to the indicator function, whose value is 1 when the condition is true; otherwise, the value is 0. ϵ refers to the decision threshold between using the trajectory sub-model and using the image sub-model.

Finally, we selected six types of UFAs from the recognition results, and they represent social production and activities, namely schools, residential areas, traffic centers, hospitals, scenic spots, and shopping malls (Figure 3).

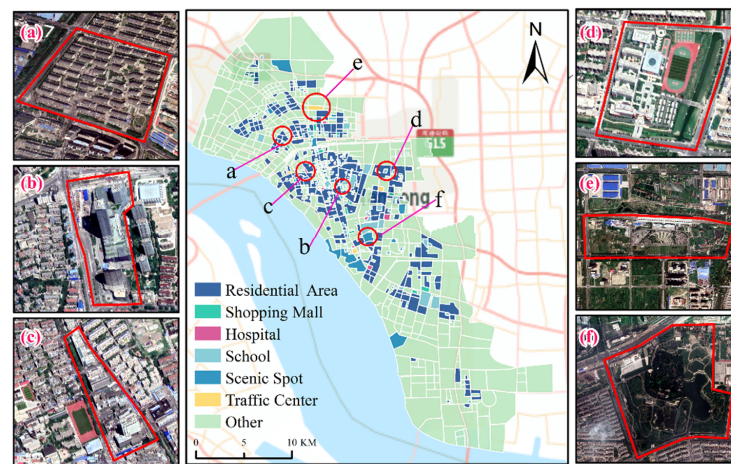


Figure 3. Identification of attributes of UFAs. (a) Residential area. (b) Shopping mall. (c) Hospital. (d) School. (e) Traffic center. (f) Scenic spot. UFAs refer to the urban functional areas.

2.3.3. Establishment of Residential Travel Structure

Residential travel structure refers to the distribution of OD points and the proportion of travel with a certain purpose in all trips. The OD matrix was first built to represent the traffic volume between the origin (O) point and the destination (D) point lying in different UFAs during a certain stage. Secondly, the O point and the D point in one trajectory were marked with different attributes of UFAs. Thirdly, the travel purposes of the OD flow were divided into commuting travel, flexible travel, and random flexible travel. Flexible travel includes shopping travel, business travel, medical travel, and tourism travel. Shopping travel and tourism travel belong to entertainment and can reflect the changes in residential entertainment activities before and after the COVID-19 outbreak. Random elastic travel

refers to travel with irregular space and time, such as the residential flow from hospitals to scenic spots. The classification of residential flows with different purposes is shown in Table 1. Finally, the proportion of OD flows with different purposes in the total volume could be calculated.

Table 1. Division of the residential travel purpose.

O \ D	School	Residential Area	Shopping Mall	Traffic Center	Hospital	Scenic Spot
School	—	Commuting travel	Random elastic travel	Random elastic travel	Random elastic travel	Random elastic travel
Residential Area	Commuting travel	—	Shopping	Business travel	Medical travel	Tourism travel
Shopping Mall	Random elastic travel	Shopping	—	Random elastic travel	Random elastic travel	Random elastic travel
Traffic Center	Random elastic travel	Business travel	Random elastic travel	—	Random elastic travel	Random elastic travel
Hospital	Random elastic travel	Medical travel	Random elastic travel	Random elastic travel	—	Random elastic travel
Scenic Spot	Random elastic travel	Tourism travel	Random elastic travel	Random elastic travel	Random elastic travel	—

O represents the origin point in one trajectory. D represents the destination point in one trajectory.

Therefore, the elements of the residential travel structure include the OD points, the flows between different UFAs, and the proportions of each type of residential flow. The OD points represent the starting and destination points in residential travel, and the flow refers to the residential flux with different purposes divided by the UFA attributes of the O and D points. The OD matrix established in this study is shown below.

$$A = \begin{bmatrix} Element_{1,1} & Element_{1,2} & Element_{1,3} & \cdots & Element_{1,m} \\ Element_{2,1} & Element_{2,2} & Element_{2,3} & \cdots & Element_{2,m} \\ Element_{3,1} & Element_{3,2} & Element_{3,3} & \cdots & Element_{3,m} \\ \vdots & \vdots & \vdots & \ddots & \vdots \\ Element_{m,1} & Element_{m,2} & Element_{m,3} & \cdots & Element_{m,m} \end{bmatrix} \tag{3}$$

where A represents the matrix of residential travel flow between different UFAs, $Element_m$ represents the type of UFA, and $Element_{i,m}$ represents the volume of residential travel between the type- i and the type- m of UFA.

2.3.4. Extraction of Hotspots of Residential Travel

The hotspots of residential travel were extracted using kernel density estimation [49]. This method takes a point in space as the center of a circle and calculates the probability density of events in a circular range of radius r . The calculation formula is as follows:

$$\lambda(s) = \sum_{i=1}^n \frac{1}{\pi r^2} k\left(\frac{d_{is}}{r}\right) \tag{4}$$

where $\lambda(s)$ represents the density at position s , d_{is} is the Euclidean distance between event point i and event point s , $k()$ is the kernel function (in this study we use the Gaussian kernel function), r is the bandwidth, and n is the total number of event points within the range of r away from s .

2.3.5. Overall Residential Travel Pattern of UFAs

The net flow rate (NFR) indicator [50], which is the net flow per unit area, analyzes the overall residential travel pattern of different types of UFAs. The higher the absolute value of NFR, the more mobile the residents that correspond to this type of UFAs are. A

positive NFR indicates that the outflow number is greater than the inflow of the same UFA during a certain period. The NFR of different types of UFA is defined as follows.

$$NFR_i = \frac{outflow_i - inflow_i}{area_i} \quad (5)$$

where NFR_i represents the NFR of i th UFA, i represents the unique identifier of each UFA, $outflow_i$ and $inflow_i$ represent the flow of residents leaving or moving into the i th UFA during a certain period, and $area_i$ represents the area of the i th UFA.

3. Results

3.1. Analysis of the Temporal Characteristics of Residential Travel Volume

3.1.1. Monthly Change in Volume of Residential Travel

Affected by COVID-19, the volume of residential travel reduced continuously from December 2019 to February 2020, then rebounded in March 2020 when the risk of COVID-19 transmission decreased, as shown in Figure 4. In January, the government formulated a timely prevention and control policy at the beginning of the COVID-19 outbreak, such as closing entertainment venues and scenic spots, and calling on residents to reduce unnecessary travel through home isolation [51]. Therefore, there was a sharp decrease in the volume of residential travel compared with the same period of the previous year. Moreover, the difference between the day with the largest travel volume and the day with the lowest travel volume reached the maximum, indicating that residential travel disorder was at a high level. With the strict enforcement of control policy in all aspects, there was a minimum difference between the day with the largest volume and the day with the lowest travel volume in February 2020, indicating that residential travel was highly orderly. However, the median of the volume of residential travel in March 2020 was significantly higher than that in February, and the difference between the maximal and minimal travel volume increased greatly compared with February, indicating that the volume of residential travel improved. With the decreasing transmission risk, although the volume of residential travel began to increase, there was still a gap compared with the normal behavior of society, indicating that society was still in a steady state of recovery.

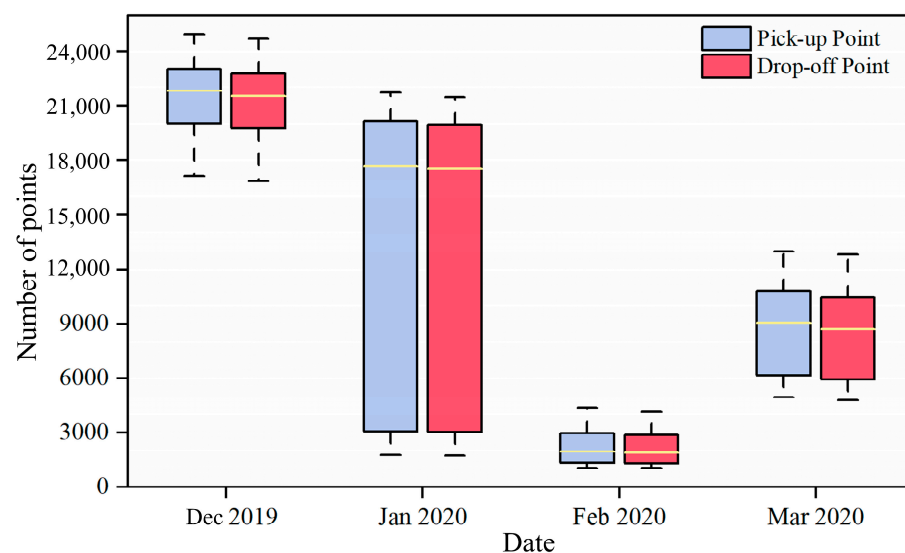


Figure 4. Monthly change in residential travel volume.

3.1.2. Daily Change in Volume of Residential Travel

The daily volume of residential travel from December 2019 to March 2020 was measured to explore certain time nodes and sudden changes throughout the period from the outbreak to the gradual recovery of the society, as shown in Figure 5.

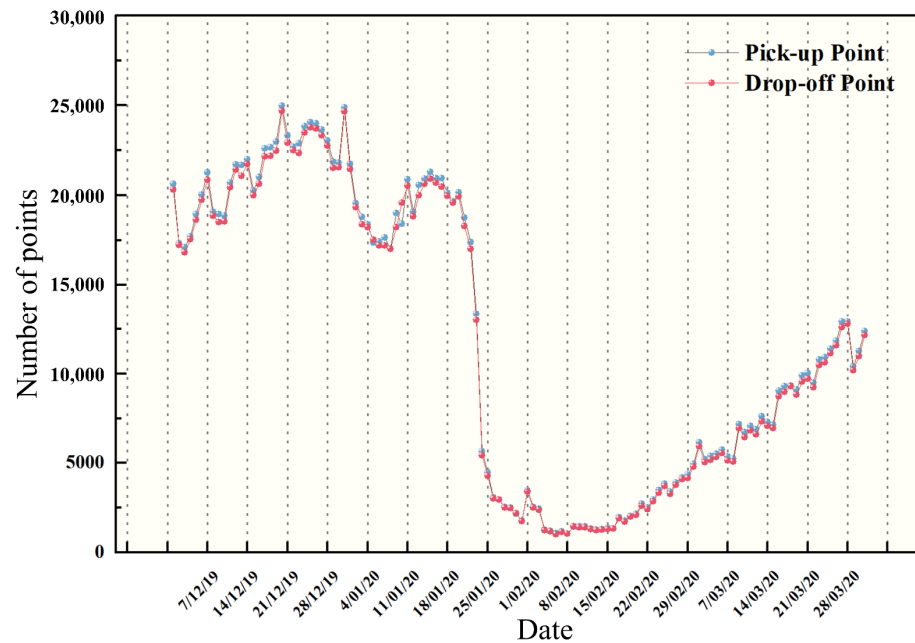


Figure 5. Daily change in residential travel volume.

The volume of residential travel fluctuated back and forth in December 2019 because people had incomplete knowledge of the rapid spread and severe explosiveness of the pandemic. Due to travel control measures, there was a significant downward trend from 1 January to 8 February 2020. The volume rebounded until 9 February 2020, and increased substantially in March 2020 when the pandemic was under control and society gradually returned to normal.

3.1.3. Period Division of COVID-19

Some events may have had a certain impact on the spread of COVID-19 in Nantong City, Jiangsu Province, including the first report of unexplained pneumonia in Wuhan city, the first confirmed case of COVID-19 in Nantong city, the reopening of the first batch of enterprises and factories in Nantong city, the opening of recreation places such as scenic spots and shopping centers, and many other nodes [52,53]. To more scientifically and reasonably reveal the changes in residential travel structure, the spread of COVID-19 was divided into five periods: normal period of society, early period of COVID-19, outbreak period of COVID-19, rework period of society, and recovery period of society, as shown in Figure 6.

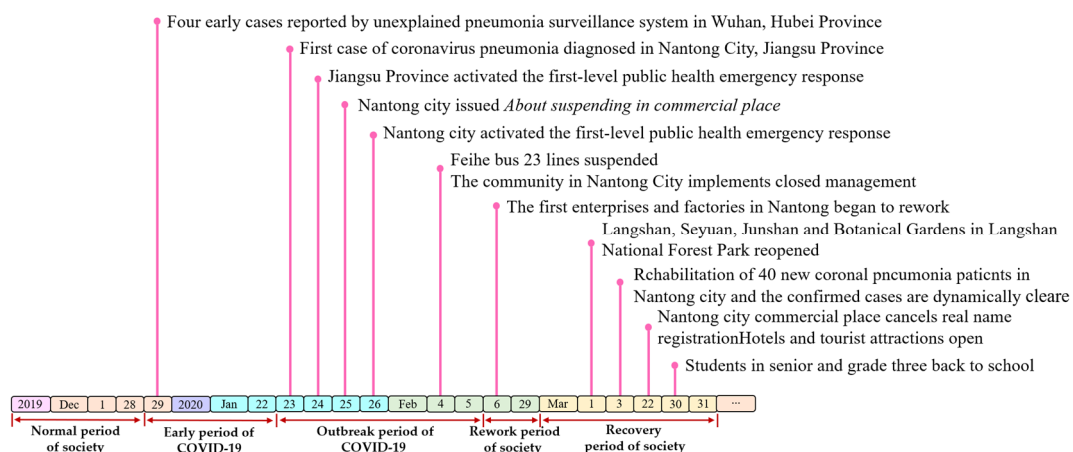


Figure 6. Major events during the transmission period of COVID-19.

3.2. Analysis of the Spatial Change in Residential Travel Volume

3.2.1. Hotspot Changes in Residential Travel

From the early stage to the outbreak period of COVID-19, the number of hotspots of residential travel significantly decreased and the spatial distribution range sharply dropped compared with that in the normal period (Figure 7a–c). In the rework period of society, the number of hotspots of residential travel remained low, as well as the hotspots mainly gathered near the residential areas (Figure 7d). This preliminarily proved that commuting travel accounted for a relatively high proportion of other kinds of residential travel with different purposes during COVID-19. In the recovery period of society, hotspots of residential travel gradually expanded outward from the urban central areas, as shown in Figure 7e. The number of hotspots of residential travel increased and the scope expanded, but there was still a certain gap compared with the normal period of society.

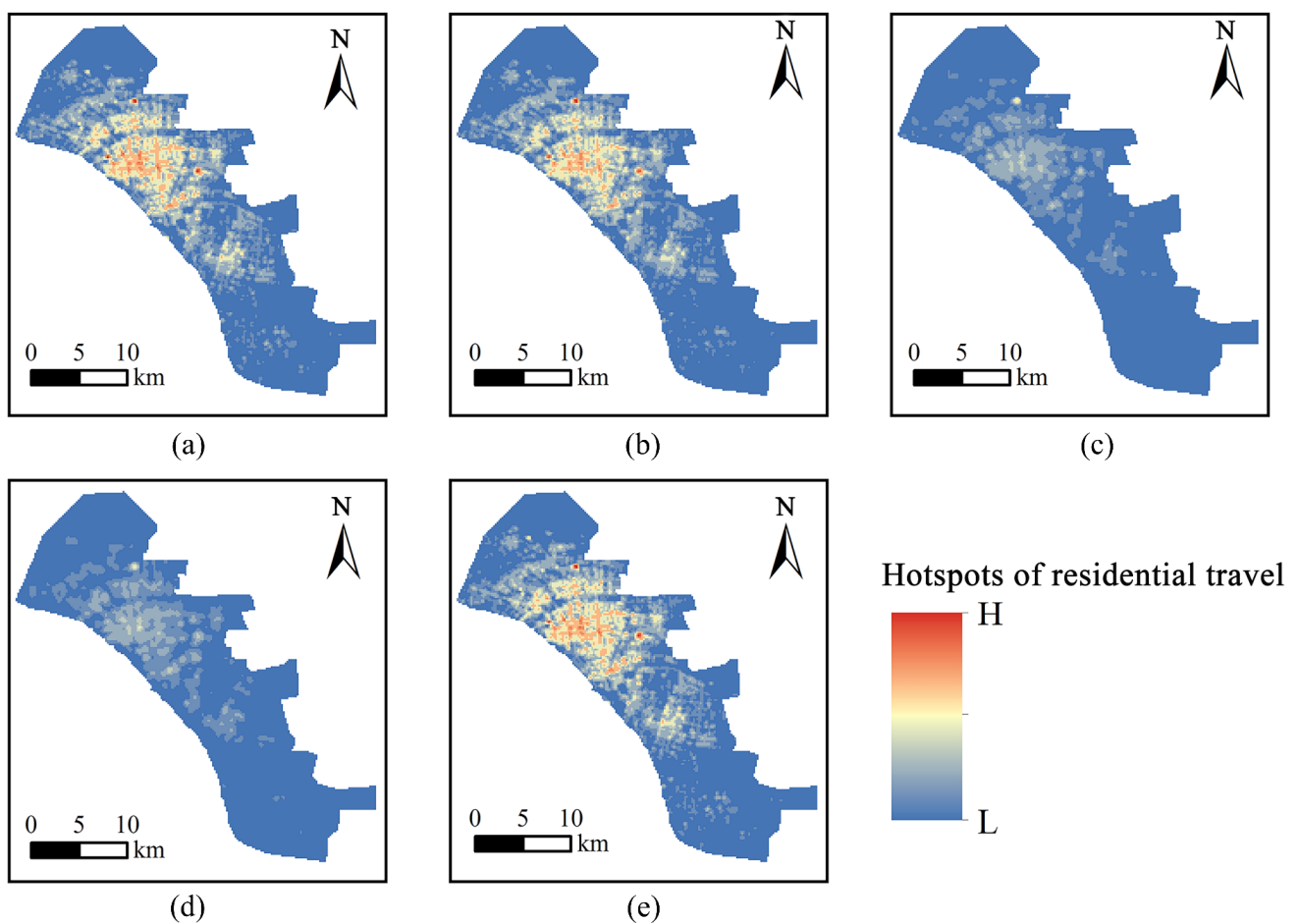


Figure 7. Urban hotspots of residential travel in (a) normal period of society, (b) early period of COVID-19, (c) outbreak period of COVID-19, (d) rework period of society, and (e) recovery period of society.

3.2.2. Coupling Analysis of OD Points and Marked Points with Attributes of UFAs

To explore the distribution changes in OD points around various UFAs, the number of pick-up and drop-off points within $1 \text{ km} \times 1 \text{ km}$ grid were counted during COVID-19. The number of points decreased and the points moved from the suburbs to the main urban area, indicating that the travel scope of residents has narrowed and has been primarily concentrated in the center of the main city since the outbreak of COVID-19.

The saturation of color indicates the density of OD points around each UFA in different periods. Affected by COVID-19, the density of O points around traffic centers, scenic spots,

and shopping malls was significantly reduced. In the outbreak period, the density of O points around schools, residential areas, and hospitals was at a relatively high level. As society gradually returned to normal, the density of O points around various UFAs also gradually increased (Figure 8). During the outbreak period, the density of D points around the traffic centers, scenic spots, and shopping centers was at a low level, and the dense area of D points was mainly distributed around hospitals, schools, and residential communities (Figure 9). In summary, the density of residential travel around hospitals, schools, and residential areas was high and maintained a low level around other types of marked points, which could preliminarily indicate the change in the residential travel structure and commuting, and medical travel occupied a high proportion of the total travel volume during the pandemic period.

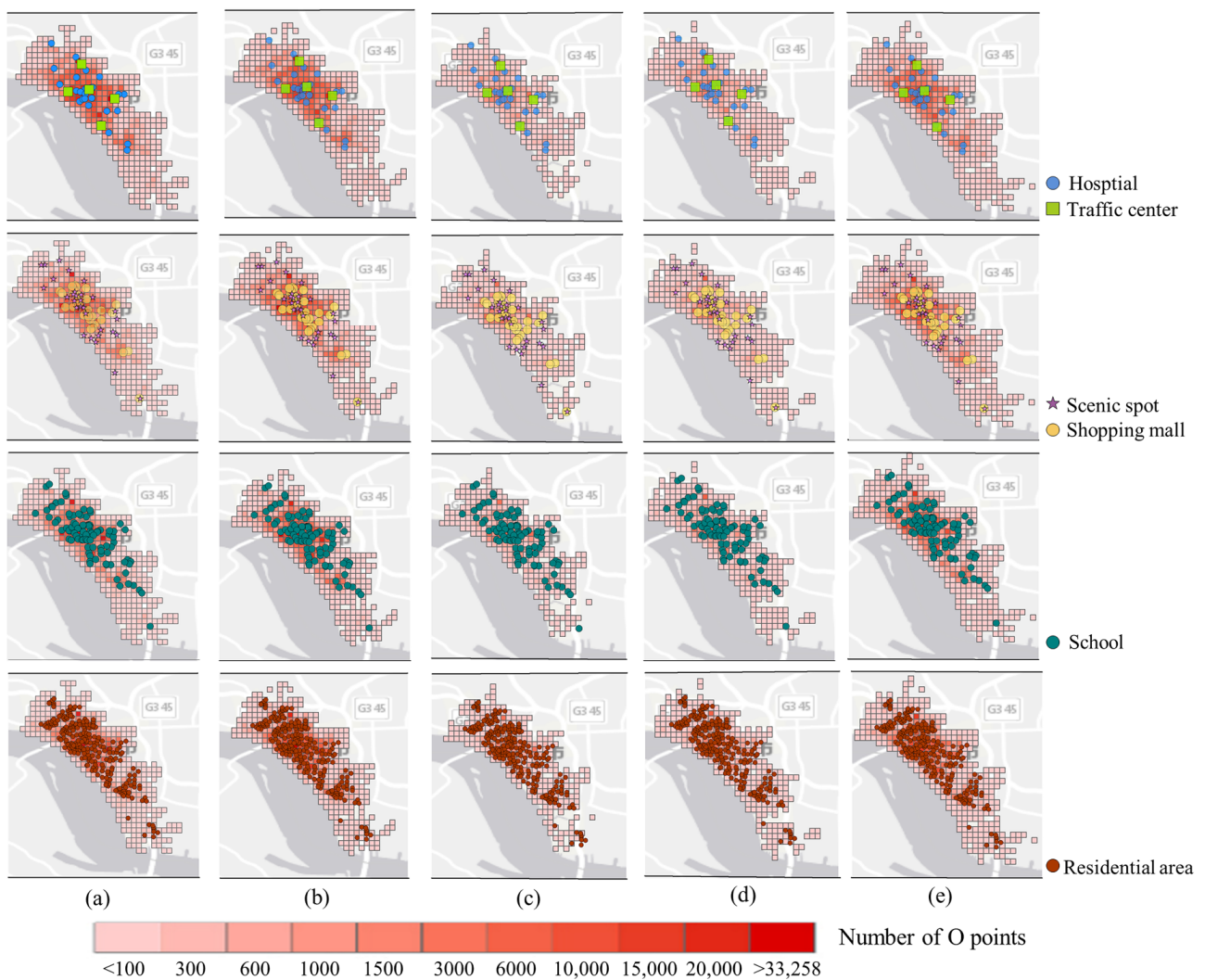


Figure 8. The density of O points around each UFA in (a) normal period of society, (b) early period of COVID-19, (c) outbreak period of COVID-19, (d) rework period of society, and (e) recovery period of society. O point represents the origin point in one trajectory of residential travel. Marked points were obtained from the center points of UFAs. The size of the grid is 1 km \times 1 km.

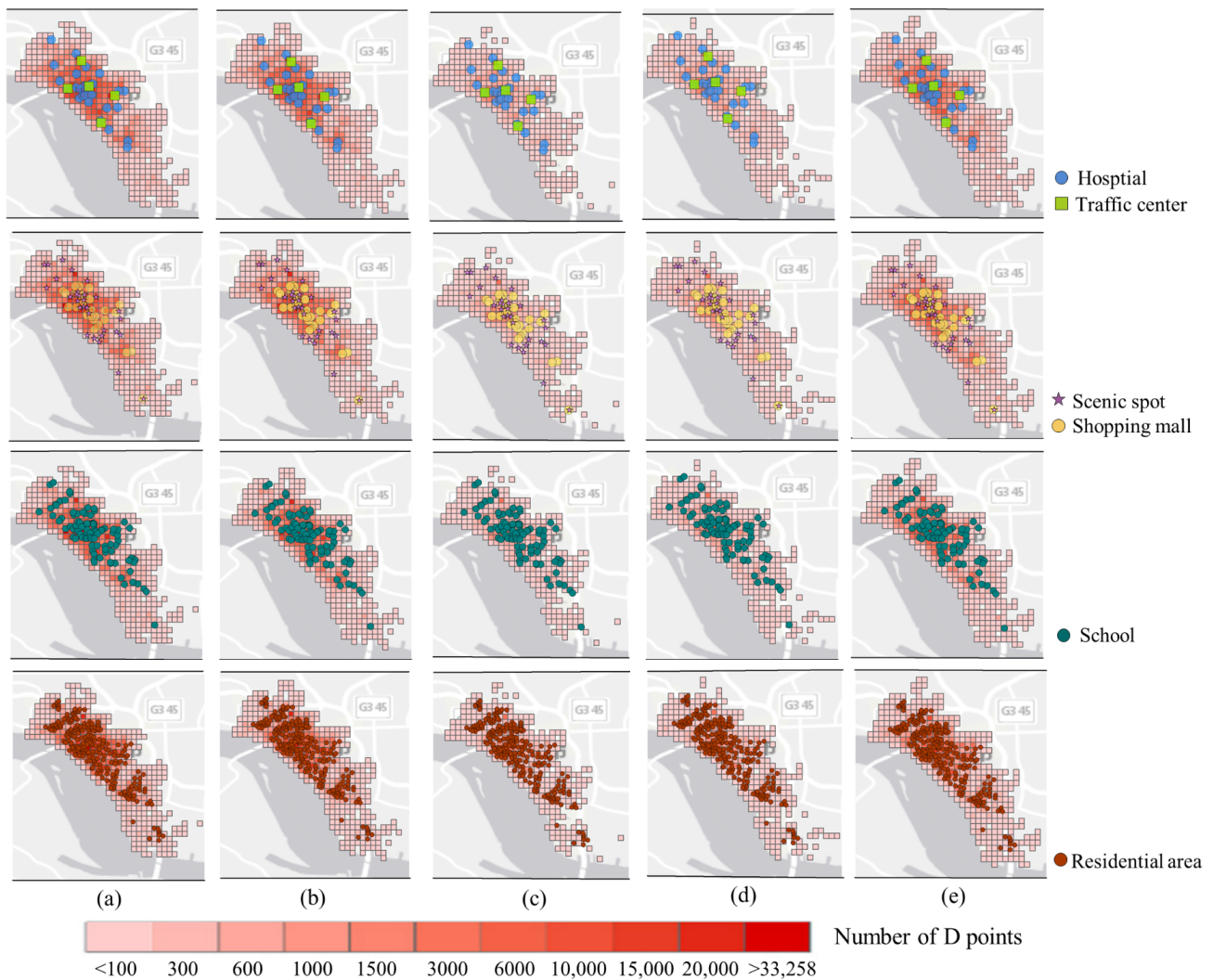


Figure 9. The density of D points around each UFA in (a) normal period of society, (b) early period of COVID-19, (c) outbreak period of COVID-19, (d) rework period of society, and (e) recovery period of society. D point represents the destination point in one trajectory of residential travel. Marked points were obtained from the center points of UFAs. The size of the grid is 1 km \times 1 km.

3.3. Analysis of Changes in Residential Travel Flow and Travel Purpose

3.3.1. Changes in Residential Travel Flow over Different Periods

In the normal period of society before COVID-19, commuting travel and business travel accounted for a higher proportion than other types of residential travel (Figure 10a). In the early period of COVID-19, the proportion of commuting travel decreased, but the proportion of other types of residential travel increased (Figure 10b). This was due to the fact that it coincided with the eve of the Spring Festival and the awareness of the great risk of COVID-19 was generally low. Until the outbreak period, the proportions of other types of residential travel except commuting travel and medical travel decreased, especially the proportions of shopping travel and tourism travel (Figure 10c). This indicated that residents only retained their travel behavior to meet basic survival needs. The proportions of shopping travel and tourism travel increased in the rework period (Figure 10d) and then decreased in the recovery period (Figure 10e), indicating that there was strong demand for entertainment as the risk of the spread of COVID-19 had been reduced (Figure 6). The proportions of business travel and random elastic travel decreased to the lowest levels during the rework period, indicating that society was still in a highly orderly state and the awareness of the pandemic still remained high. In the recovery period of society, the

proportion of business travel significantly increased due to the relaxation of government measures. The proportion of medical travel increased in the early period of COVID-19, the outbreak period of COVID-19, and the recovery period of society, so we can refer to the proportion of residential travel structures to evaluate the health status of different cities, which is helpful for the sustainable development of cities.

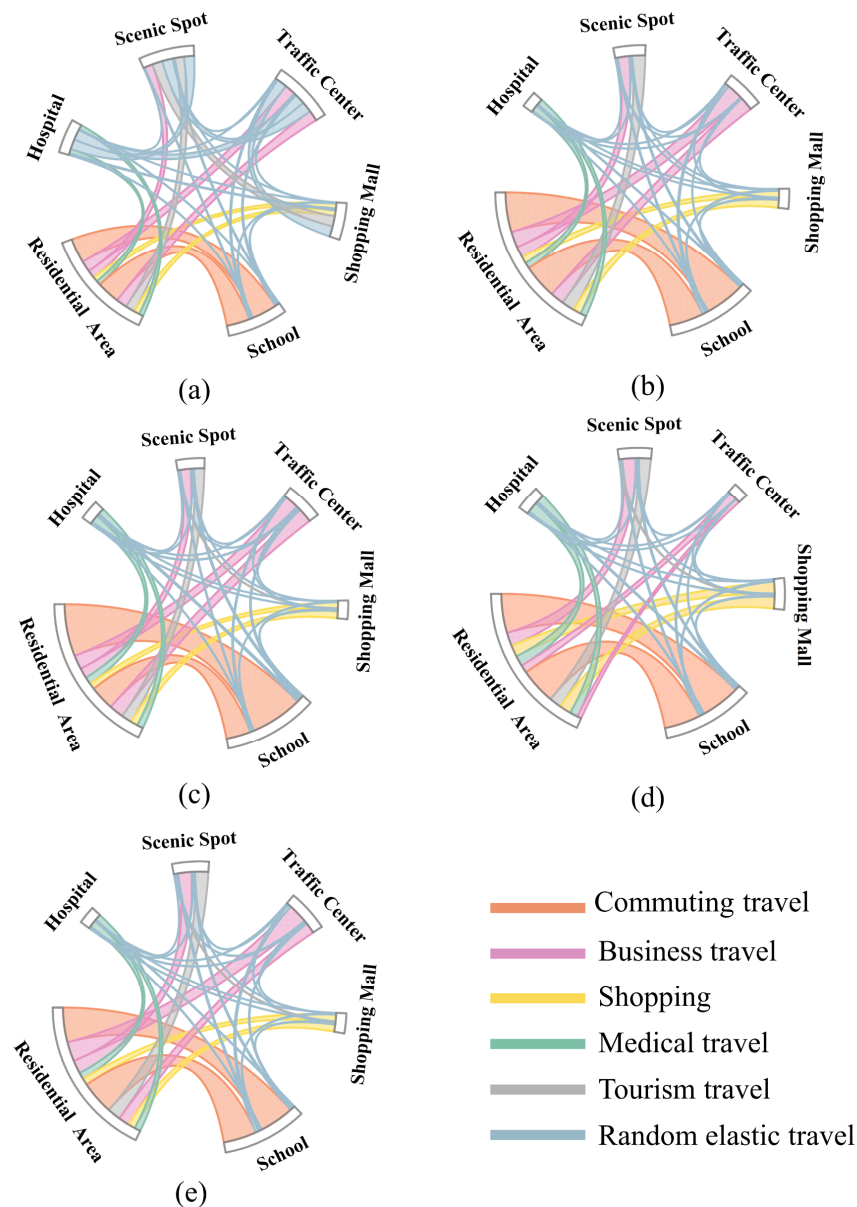


Figure 10. Residential travel flow in (a) normal period of society, (b) early period of COVID-19, (c) outbreak period of COVID-19, (d) rework period of society, and (e) recovery period of society.

The NFR indicator was used to analyze the overall flow pattern of residential travel of different types of UFAs (Figure 11). The absolute values of the NFRs of scenic spots and schools showed that residential mobility in these UFAs was at a low level under the policy of closing scenic spots and teaching online. The absolute value of the NFRs of the transportation center was always at the highest level but decreased significantly during the outbreak period because of the decrease in residential travel within and between cities under the restriction policy. The NFR of shopping centers was positive in the outbreak period of COVID-19, but negative in the rework and recovery periods of society, indicating that residents' demand for spiritual and cultural consumption changed from weak to strong

during different periods of the pandemic. Conversely, the NFR of residential areas was negative in the outbreak period and positive in the other periods. This can be explained because residents were isolated at home and took the initiative to reduce the amount of travel. Overall, the decreased absolute value of the NFR in various types of UFAs showed that the whole of residential travel exhibited a decreasing trend compared with the normal period of society under the isolation policy. After the risk of transmission was reduced, the absolute value of the NFR gradually increased and residential travel gradually returned to normal.

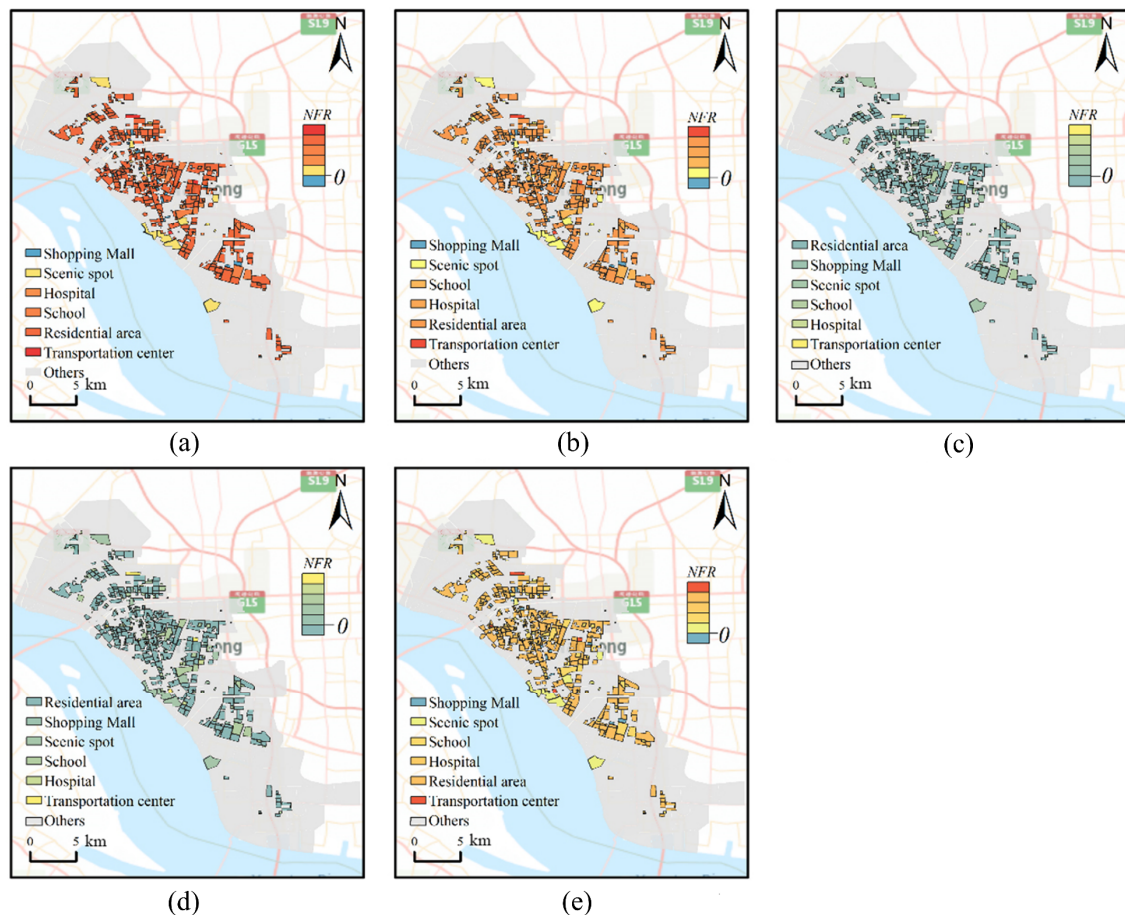


Figure 11. NFR of UFAs in (a) normal period of society, (b) early period of COVID-19, (c) outbreak period of COVID-19, (d) rework period of society, and (e) recovery period of society. NFR represents the net flow rate. UFAs represent urban functional areas.

3.3.2. Ratio of Residential Travel with Different Purposes

From the normal period to the outbreak of COVID-19, the ratios of shopping travel, business travel, tourism travel, and random elastic travel all showed a trend of first increasing and then decreasing, while the ratio of commuting travel showed a trend of decreasing first and then increasing. The ratio of medical travel continued to increase. However, from the outbreak period to the recovery period, the ratio changes in various types of residential travel showed significant differences. Taking the rework period as a turning point, the ratio of business travel and random elastic travel first decreased and then increased, and the ratio of shopping and medical travel increased first and then decreased. The ratio of tourism travel kept increasing, while that of commuting travel showed a continuous downward trend.

Overall, the ratio changes in commuting travel, random travel, and random elastic travel showed a roughly symmetrical trend in five periods of COVID-19, as shown in Figure 12.

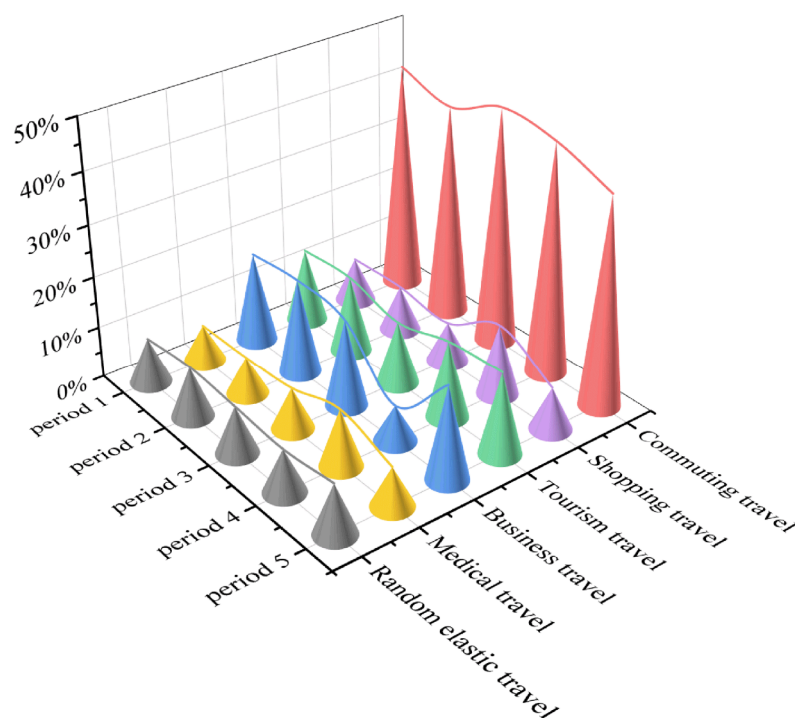


Figure 12. The ratios of residential travel with different purposes over different periods. Period 1 represents the normal period of society. Period 2 represents the early period of COVID-19. Period 3 represents the outbreak period of COVID-19. Period 4 represents the rework period of society. Period 5 represents the recovery period of society.

4. Discussion

4.1. Identification of Residential Travel Purpose

Previous studies on identifying the purpose of residential travel have only simply associated the origin and destination points with POI points. However, a variety of types of POI points are similar in space in the actual situation, and it is hard to determine the travel purpose when the trajectory points fall between multiple POI points. For example, a restaurant and small shop are located near the hospital, and the current drop-off point is located near the restaurant and the small shop, which are closer than the hospital. In this situation, the residential travel purpose is more likely to be seeking medical treatment rather than shopping and eating. In this paper, UFAs were used to improve the accuracy for the identification of travel purposes.

The POI data were collected via crawler technology combined with the API interface provided by Baidu Maps. Finally, a total of 88,331 pieces of POI data in Chongchuan District, Nantong, China were obtained. Its original data include fields such as name, category, latitude and longitude, and address, as shown in Table A1. By filtering the category fields and specifying coordinates, multiple categories of POI data can be obtained, as shown in Figure A1.

4.2. Changes in Residential Psychological Needs

According to Maslow's hierarchy of needs model, medical travel, shopping travel, and tourism travel were, respectively, classified as physiological needs, love and belonging needs, and esteem needs, while commuting travel and business travel were classified as safety needs [54], as shown in Figure 13.



Figure 13. Classification of residential travel according to Maslow’s hierarchy of needs.

From the normal period of society to the early period of COVID-19, love and belonging needs were the main demands of residents, but these demands decreased significantly after the isolation policy (Table 2). The physiological needs and safety needs were the main demands of residents during the outbreak of COVID-19, and this can be further explained by the fact that the operation of the city needed to meet these two needs during the public health emergency period. During the rework period of society, in addition to physiological needs and safety needs, love and belonging needs and esteem needs continued to rise. From the early period to the outbreak period of COVID-19, the increasing proportion of commuting and medical travel showed that the primary living demands of residents were physiological and safety needs. Only when the two basic needs of residents were met could society operate normally during an emergency. Moreover, the love and belonging needs and esteem needs of residents increased when society gradually returned to normal.

Table 2. The proportions of residential travel with different purposes over different periods.

Social Period	Commuting Travel	Shopping and Entertainment	Medical Travel	Business Travel	Tourism and Leisure	Random Elastic Travel
Period 1	43.8	8.5	7.1	17.5	14.3	8.8
Period 2	40.9	8.8	7.3	18.4	14.8	9.9
Period 3	45.7	7.7	8.1	17.0	12.2	9.2
Period 4	44.6	13.8	11.1	7.0	15.0	8.4
Period 5	40.5	8.2	7.6	18.1	15.9	9.7

Period 1 represents the normal period of society. Period 2 represents the early period of COVID-19. Period 3 represents the outbreak period of COVID-19. Period 4 represents the rework period of society. Period 5 represents the recovery period of society.

4.3. Comparison with Previous Studies

Compared with previous studies, the advancement of this paper is mainly reflected in three aspects: (1) Based on FCD data, the location and duration of residential travel can be accurately obtained, while previous studies mostly used questionnaires [55] or mobile phone signal data [56]. However, questionnaires are too subjective because the respondents may not pay the necessary attention to them during the response process. Similarly, mobile phone signaling data cannot record the integrity of the travel path. (2) Regarding the purpose identification of travelers, previous studies mostly used the distance from the POI data to determine the attribution of the drop-off points [27], but sometimes there may be multiple types of POI data around the drop-off point, which affects the recognition effect. The proposed method based on UFA reduces the error to a certain extent compared to the traditional method. (3) For the first time, this paper integrates Maslow’s theory of psychological needs into the study of spatiotemporal changes in residential travel. This attempt is interdisciplinary research in the fields of geography, transportation, and society, which will help improve the methodology system of residential travel from multiple perspectives.

There are still some limitations in this paper. Firstly, only taxi trajectory data were used to analyze the residential travel structure. However, there remain other travel methods in a sustainable city system, such as public buses, subways, shared bicycles, and walking. In order to understand the travel characteristics more comprehensively, multiple dimensions should be considered together in future studies on residential travel behavior [57]. In addition, other social sensing data, such as smartphone data, can be used to improve the identification of residential travel purposes. Secondly, this experiment was conducted only on the scale of a single city, while the changes in the residential travel structure in a megacity inevitably have an impact on neighboring satellite cities. To explore the synergistic relationship between the travel structure changes among cities at different development levels, future studies should focus on the urban agglomeration or regional scale.

5. Conclusions

In this research, we used taxi trajectory data combined with multi-source data to analyze the impact of COVID-19 on the residential travel structure of Nantong, China. The following results were obtained. (1) Compared with the normal period of society, the volume of residential travel continued to decline and the hotspots decreased from the suburbs to the main urban area. (2) The absolute values of NFR for all types of UFAs showed a decreasing trend during the early period and outbreak period and the residential travel gradually returned to normal until the epidemic was controlled. (3) Although the ratios of commuting travel, random travel, and random elastic varied at different periods, they showed a roughly symmetrical trend across the process. (4) The needs of residents were mainly physiological and safety-related during the outbreak period. Love and belonging needs and esteem needs increased when society gradually returned to normal.

The main significance of this study lies in two aspects. Academically, a method to establish the residential travel structure was constructed, which can provide suggestions for urban sustainable development. Moreover, the findings have important practical significance. By understanding the spatiotemporal changes in the density and proportions of residential travel, decision makers can take appropriate actions to mitigate the impacts of major public health emergencies, which will lay the foundation for more informed and effective policies.

Author Contributions: Conceptualization, Fei Tao and Tong Zhou; methodology, Fei Tao and Tong Zhou; software, Junjie Wu and Shuang Lin; validation, Yaqiao Lv, Yu Wang and Junjie Wu; formal analysis, Junjie Wu and Shuang Lin; investigation, Yu Wang and Fei Tao; data curation, Fei Tao and Yu Wang; writing—original draft preparation, Fei Tao and Tong Zhou; writing—review and editing, Fei Tao, Tong Zhou and Junjie Wu; visualization, Shuang Lin and Yaqiao Lv; supervision, Tong Zhou; project administration, Fei Tao; funding acquisition, Fei Tao and Tong Zhou. All authors have read and agreed to the published version of the manuscript.

Funding: This research was funded by the National Natural Science Foundation of China (42271451), in part by the Natural Science and Technology Project of Nantong (MS12021082), in part by Industry-University Cooperation Collaborative Education Projects (202102245013), the National College Students Innovation and Entrepreneurship Training Program (202210304054Z, 202210304057Z), and the Jiangsu Province College Students Innovation and Entrepreneurship Training Program (202210304141Y).

Data Availability Statement: Not applicable.

Acknowledgments: We would like to thank the editor and the anonymous reviewers who provided insightful comments on improving this paper. We also would like to thank domestic software Pixel Information Expert (PIE) for their commitment to remote sensing applications that have driven the progress of this study.

Conflicts of Interest: The authors declare no conflict of interest.

Appendix A

Table A1. Samples of the POI data derived from the web crawler.

Name	Category	Longitude and Latitude (°)	Address
Sinopec Nantong South Gongnong Road Gas Station	Car service; Gas station; SINOPEC	120.885892780469, 31.9702633794535	No. 26, Taoyuan Road
Sinopec Nantong Huaqiang Gas Station	Car service; Gas station; SINOPEC	120.884506906742, 31.9961696011873	North side of the social welfare home, Jiangwei Road
PetroChina Langshan Gas Station (Changjiang South Road)	Car service; Gas station; PetroChina	120.87968132384, 31.9652934384395	211 Changjiang South Road
⋮	⋮	⋮	⋮
⋮	⋮	⋮	⋮
Building 4, dormitory of smoke filter experimental factory	Place name address information; House number information; Building pillar number	120.841293438875, 32.0265615923866	50 m to the west at the intersection of Hai'er Lane North Road and Haobei Road
Public lavatory	Public facilities; Public facilities; Public facilities	120.848458282361, 32.0270879262701	Near Haobei Road

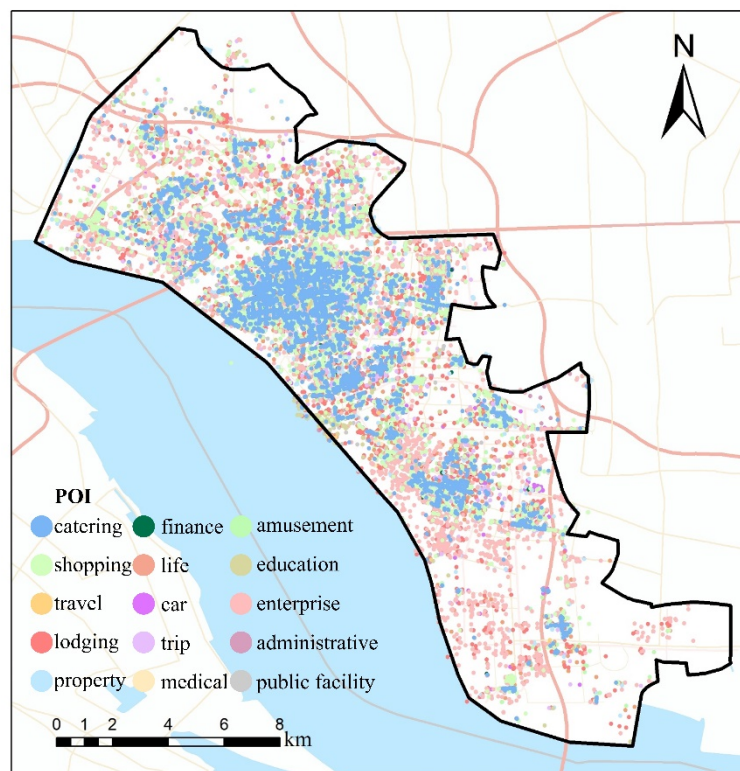


Figure A1. Thematic map of the classified POI data.

References

- Lu, H.; Stratton, C.W.; Tang, Y.-W. Outbreak of pneumonia of unknown etiology in Wuhan, China: The mystery and the miracle. *J. Med. Virol.* **2020**, *92*, 401–402. [\[CrossRef\]](#)
- Karim, A.; Akter, M.; Mazid, T.; Pulock, O.S.; Aziz, T.T.; Hayee, S.; Tamanna, N.; Chuwdhury, G.S.; Haque, A.; Yeasmin, F.; et al. Knowledge and Attitude towards COVID-19: A Cross Sectional Study in Bangladesh through Phone and Online Survey. *J. Clin. Exp. Investig.* **2020**, *11*, em00757. [\[CrossRef\]](#)
- Tay, M.Z.; Poh, C.M.; Rénia, L.; Macary, P.A.; Ng, L.F.P. The trinity of COVID-19: Immunity, inflammation and intervention. *Nat. Rev. Immunol.* **2020**, *20*, 363–374. [\[CrossRef\]](#)
- Sun, C.; Zhai, Z. The efficacy of social distance and ventilation effectiveness in preventing COVID-19 transmission. *Sustain. Cities Soc.* **2020**, *62*, 102390. [\[CrossRef\]](#)
- Sen-Crowe, B.; McKenney, M.; Elkbuli, A. Social distancing during the COVID-19 pandemic: Staying home save lives. *Am. J. Emerg. Med.* **2020**, *38*, 1519–1520. [\[CrossRef\]](#)
- Paul, A.; Chatterjee, S.; Bairagi, N. Prediction on Covid-19 epidemic for different countries: Focusing on South Asia under various precautionary measures. *Medrxiv* **2020**. [\[CrossRef\]](#)

7. Lin, Q.; Zhao, S.; Gao, D.; Lou, Y.; Yang, S.; Musa, S.S.; Wang, M.H.; Cai, Y.; Wang, W.; Yang, L.; et al. A conceptual model for the coronavirus disease 2019 (COVID-19) outbreak in Wuhan, China with individual reaction and governmental action. *Int. J. Infect. Dis.* **2020**, *93*, 211–216. [[CrossRef](#)]
8. Couto, G.; Castanho, R.; Pimentel, P.; Carvalho, C.; Sousa, A.; Santos, C. The Impacts of COVID-19 Crisis over the Tourism Expectations of the Azores Archipelago Residents. *Sustainability* **2020**, *12*, 7612. [[CrossRef](#)]
9. Jung, H.-S.; Yoon, H.-H.; Song, M.-K. A Study on Dining-Out Trends Using Big Data: Focusing on Changes since COVID-19. *Sustainability* **2021**, *13*, 11480. [[CrossRef](#)]
10. Wesolowski, A.; Eagle, N.; Tatem, A.J.; Smith, D.L.; Noor, A.M.; Snow, R.W.; Buckee, C.O. Quantifying the Impact of Human Mobility on Malaria. *Science* **2012**, *338*, 267–270. [[CrossRef](#)]
11. Liu, Y.; Liu, X.; Gao, S.; Gong, L.; Kang, C.; Zhi, Y.; Chi, G.; Shi, L. Social Sensing: A New Approach to Understanding Our Socioeconomic Environments. *Ann. Assoc. Am. Geogr.* **2015**, *105*, 512–530. [[CrossRef](#)]
12. Yuan, N.J.; Zheng, Y.; Xie, X.; Wang, Y.; Zheng, K.; Xiong, H. Discovering Urban Functional Zones Using Latent Activity Trajectories. *IEEE Trans. Knowl. Data Eng.* **2015**, *27*, 712–725. [[CrossRef](#)]
13. Li, H.; Zhang, Y.; Zhu, M.; Ren, G. Impacts of COVID-19 on the usage of public bicycle share in London. *Transp. Res. Part A Policy Pract.* **2021**, *150*, 140–155. [[CrossRef](#)]
14. Tiikkaja, H.; Viri, R. The effects of COVID-19 epidemic on public transport ridership and frequencies. A case study from Tampere, Finland. *Transp. Res. Interdiscip. Perspect.* **2021**, *10*, 100348. [[CrossRef](#)]
15. Liu, R.; Tao, F.; Liu, X.; Na, J.; Leng, H.; Wu, J.; Zhou, T. RANet: A Residual ASPP with Attention Framework for Semantic Segmentation of High-Resolution Remote Sensing Images. *Remote. Sens.* **2022**, *14*, 3109. [[CrossRef](#)]
16. Ma, P.; Tao, F.; Gao, L.; Leng, S.; Yang, K.; Zhou, T. Retrieval of Fine-Grained PM2.5 Spatiotemporal Resolution Based on Multiple Machine Learning Models. *Remote. Sens.* **2022**, *14*, 599. [[CrossRef](#)]
17. Aloï, A.; Alonso, B.; Benavente, J.; Cordera, R.; Echániz, E.; González, F.; Ladisa, C.; Lezama-Romanelli, R.; López-Parra, Á.; Mazzei, V.; et al. Effects of the COVID-19 Lockdown on Urban Mobility: Empirical Evidence from the City of Santander (Spain). *Sustainability* **2020**, *12*, 3870. [[CrossRef](#)]
18. Wilbur, M.; Ayman, A.; Ouyang, A.; Poon, V.; Kabir, R.; Vadali, A.; Pugliese, A.; Freudberg, D.; Laszka, A.; Dubey, A. Impact of COVID-19 on public transit accessibility and ridership. *arXiv* **2020**, arXiv:2008.02413. [[CrossRef](#)]
19. Hua, M.; Chen, X.; Cheng, L.; Chen, J. Should bike-sharing continue operating during the COVID-19 pandemic? Empirical findings from Nanjing, China. *J. Transp. Health* **2021**, *23*, 101264. [[CrossRef](#)]
20. Liu, J.; Li, Q.; Qu, M.; Chen, W.; Yang, J.; Xiong, H.; Zhong, H.; Fu, Y. Station Site Optimization in Bike Sharing Systems. In Proceedings of the 2015 IEEE International Conference on Data Mining, Atlantic City, NJ, USA, 14–17 November 2015; pp. 883–888.
21. Orro, A.; Novales, M.; Monteagudo, Á.; Pérez-López, J.-B.; Bugarín, M. Impact on City Bus Transit Services of the COVID-19 Lockdown and Return to the New Normal: The Case of A Coruña (Spain). *Sustainability* **2020**, *12*, 7206. [[CrossRef](#)]
22. Sun, D.; Ding, X. Spatiotemporal evolution of ridesourcing markets under the new restriction policy: A case study in Shanghai. *Transp. Res. Part A Policy Pract.* **2019**, *130*, 227–239. [[CrossRef](#)]
23. Sun, D.; Zhang, K.; Shen, S. Analyzing spatiotemporal traffic line source emissions based on massive didi online car-hailing service data. *Transp. Res. Part D Transp. Environ.* **2018**, *62*, 699–714. [[CrossRef](#)]
24. Fu, X.; Sun, M.; Sun, H. Taxi commute recognition and temporal-spatial characteristics analysis based on GPS data. *China J. Highw. Transp.* **2017**, *30*, 134.
25. Shen, X.; Zhou, Y.; Jin, S.; Wang, D. Spatiotemporal influence of land use and household properties on automobile travel demand. *Transp. Res. Part D Transp. Environ.* **2020**, *84*, 102359. [[CrossRef](#)]
26. Gao, L.; Tao, F.; Liu, R.; Wang, Z.; Leng, H.; Zhou, T. Multi-scenario simulation and ecological risk analysis of land use based on the PLUS model: A case study of Nanjing. *Sustain. Cities Soc.* **2022**, *85*, 104055. [[CrossRef](#)]
27. Xing, Y.; Wang, K.; Lu, J.J. Exploring travel patterns and trip purposes of dockless bike-sharing by analyzing massive bike-sharing data in Shanghai, China. *J. Transp. Geogr.* **2020**, *87*, 102787. [[CrossRef](#)]
28. Furlletti, B.; Cintia, P.; Renso, C.; Spinsanti, L. Inferring human activities from GPS tracks. In Proceedings of the 2nd ACM SIGKDD International Workshop on Urban Computing, Chicago, IL, USA, 11 August 2013. [[CrossRef](#)]
29. Cui, Y.; Meng, C.; He, Q.; Gao, J. Forecasting current and next trip purpose with social media data and Google Places. *Transp. Res. Part C Emerg. Technol.* **2018**, *97*, 159–174. [[CrossRef](#)]
30. Luo, X.; Cottam, A.; Wu, Y.-J.; Jiang, Y. Hybrid-Data Approach for Estimating Trip Purposes. *Transp. Res. Rec. J. Transp. Res. Board* **2021**, *2675*, 545–553. [[CrossRef](#)]
31. Zhang, X.; Sun, Y.; Zheng, A.; Wang, Y. A New Approach to Refining Land Use Types: Predicting Point-of-Interest Categories Using Weibo Check-in Data. *ISPRS Int. J. Geo-Information* **2020**, *9*, 124. [[CrossRef](#)]
32. Long, Y.; Liu, X. Featured Graphic. How Mixed is Beijing, China? A Visual Exploration of Mixed Land Use. *Environ. Plan. A Econ. Space* **2013**, *45*, 2797–2798. [[CrossRef](#)]
33. Bick, A.; Blandin, A.; Mertens, K. Work from home after the COVID-19 outbreak. *SSRN Electron* **2020**. [[CrossRef](#)]
34. Brynjolfsson, E.; Horton, J.; Ozimek, A.; Rock, D.; Sharma, G.; TuYe, H.-Y. COVID-19 and Remote Work: An Early Look at US Data; National Bureau of Economic Research: Cambridge, MA, USA, 2020. [[CrossRef](#)]

35. Savini, L.; Candeloro, L.; Calistri, P.; Conte, A. A Municipality-Based Approach Using Commuting Census Data to Characterize the Vulnerability to Influenza-Like Epidemic: The COVID-19 Application in Italy. *Microorganisms* **2020**, *8*, 911. [[CrossRef](#)]
36. Terziyska, I.; Dogramadjieva, E. Should I stay or should I go? Global COVID-19 pandemic influence on travel intentions of Bulgarian residents. *SHS Web Conf.* **2021**, *92*, 01048. [[CrossRef](#)]
37. Rahman, M.K.; Gazi, M.A.I.; Bhuiyan, M.A.; Rahaman, M.A. Effect of Covid-19 pandemic on tourist travel risk and management perceptions. *PLoS ONE* **2021**, *16*, e0256486. [[CrossRef](#)]
38. Prentice, C.; Quach, S.; Thaichon, P. Antecedents and consequences of panic buying: The case of COVID-19. *Int. J. Consum. Stud.* **2021**, *46*, 132–146. [[CrossRef](#)]
39. Chopdar, P.K.; Paul, J.; Prodanova, J. Mobile shoppers' response to Covid-19 phobia, pessimism and smartphone addiction: Does social influence matter? *Technol. Forecast. Soc. Chang.* **2022**, *174*, 121249. [[CrossRef](#)]
40. Cheung, C.; Takashima, M.; Choi, H.; Yang, H.; Tung, V. The impact of COVID-19 pandemic on the psychological needs of tourists: Implications for the travel and tourism industry. *J. Travel Tour. Mark.* **2021**, *38*, 155–166. [[CrossRef](#)]
41. Cascetta, E. *Transportation Systems Analysis: Models and Applications*; Springer: Berlin, Germany, 2009.
42. Malavenda, G.A.; Musolino, G.; Rindone, C.; Vitetta, A. Residential Location, Mobility, and Travel Time: A Pilot Study in a Small-Size Italian Metropolitan Area. *J. Adv. Transp.* **2020**, *2020*, 8827466. [[CrossRef](#)]
43. Russo, F.; Musolino, G. A unifying modelling framework to simulate the Spatial Economic Transport Interaction process at urban and national scales. *J. Transp. Geogr.* **2012**, *24*, 189–197. [[CrossRef](#)]
44. Comi, A.; Rossolov, A.; Polimeni, A.; Nuzzolo, A. Private Car O-D Flow Estimation Based on Automated Vehicle Monitoring Data: Theoretical Issues and Empirical Evidence. *Information* **2021**, *12*, 493. [[CrossRef](#)]
45. Nuzzolo, A.; Comi, A.; Polimeni, A. Exploring on-demand service use in large urban areas: The case of Rome. *Arch. Transp.* **2019**, *50*, 77–90. [[CrossRef](#)]
46. Li, H.; Xu, X.; Li, X.; Ma, S.; Zhang, H. Characterizing the urban spatial structure using taxi trip big data and implications for urban planning. *Front. Earth Sci.* **2021**, *15*, 70–80. [[CrossRef](#)]
47. Cooley, T.; Anderson, G.; Felde, G.; Hoke, M.; Ratkowski, A.; Chetwynd, J.; Gardner, J.; Adler-Golden, S.; Matthew, M.; Berk, A.; et al. FLAASH, a MODTRAN4-based atmospheric correction algorithm, its application and validation. *IEEE Int. Geosci. Remote Sens. Symp.* **2002**, *3*, 1414–1418.
48. Qian, Z.; Liu, X.; Tao, F.; Zhou, T. Identification of Urban Functional Areas by Coupling Satellite Images and Taxi GPS Trajectories. *Remote Sens.* **2020**, *12*, 2449. [[CrossRef](#)]
49. Hou, Z.; Zhou, Y.; Du, R. Special issue on intelligent transportation systems, big data and intelligent technology. *Transp. Plan. Technol.* **2016**, *39*, 747–750. [[CrossRef](#)]
50. Gao, Q.-L.; Li, Q.-Q.; Yue, Y.; Zhuang, Y.; Chen, Z.-P.; Kong, H. Exploring changes in the spatial distribution of the low-to-moderate income group using transit smart card data. *Comput. Environ. Urban Syst.* **2018**, *72*, 68–77. [[CrossRef](#)]
51. Huang, L.; Liu, Z.; Li, H.; Wang, Y.; Li, Y.; Zhu, Y.; Ooi, M.C.G.; An, J.; Shang, Y.; Zhang, D.; et al. The Silver Lining of COVID-19: Estimation of Short-Term Health Impacts Due to Lockdown in the Yangtze River Delta Region, China. *Geohealth* **2020**, *4*, e2020GH000272. [[CrossRef](#)]
52. Wang, Y.; Zhu, S.; Ma, J.; Shen, J.; Wang, P.; Wang, P.; Zhang, H. Enhanced atmospheric oxidation capacity and associated ozone increases during COVID-19 lockdown in the Yangtze River Delta. *Sci. Total. Environ.* **2021**, *768*, 144796. [[CrossRef](#)]
53. Bhatti, U.A.; Zeeshan, Z.; Nizamani, M.M.; Bazai, S.; Yu, Z.; Yuan, L. Assessing the change of ambient air quality patterns in Jiangsu Province of China pre-to post-COVID-19. *Chemosphere* **2022**, *288*, 132569. [[CrossRef](#)]
54. Jang, S.; Cai, L.A. Travel motivations and destination choice: A study of British outbound market. *J. Travel Tour. Mark.* **2002**, *13*, 111–133. [[CrossRef](#)]
55. Xiao, G.; Juan, Z.; Zhang, C. Detecting trip purposes from smartphone-based travel surveys with artificial neural networks and particle swarm optimization. *Transp. Res. Part C Emerg. Technol.* **2016**, *71*, 447–463. [[CrossRef](#)]
56. Lu, Z.; Long, Z.; Xia, J.; An, C. A Random Forest Model for Travel Mode Identification Based on Mobile Phone Signaling Data. *Sustainability* **2019**, *11*, 5950. [[CrossRef](#)]
57. Rindone, C. Sustainable Mobility as a Service: Supply Analysis and Test Cases. *Information* **2022**, *13*, 351. [[CrossRef](#)]

Disclaimer/Publisher's Note: The statements, opinions and data contained in all publications are solely those of the individual author(s) and contributor(s) and not of MDPI and/or the editor(s). MDPI and/or the editor(s) disclaim responsibility for any injury to people or property resulting from any ideas, methods, instructions or products referred to in the content.